Chapter 8

Investigation of the Behavior of Steel-Concrete Composite Structure with Different Design Properties Under Far-Fault and Near Fault Earthquake Records

Serkan Etli[1]

Melek Akgül[2]

Abstract

Calculations of earthquake effects can be handled in different ways in current national or international regulations. It is of great importance to consider the second-order effects of properties. After the structural modeling, the designs are completed by using the forces obtained in the section calculations made by considering the earthquake effects. Deformations due to second-order effects can cause greater damage in sections. Within the scope of this study, steel-concrete composite systems, which are produced in Eurocode norms and have remarkable features among structural systems, have been examined. The effects of considering the sensitivity coefficient in the Eurocode in the examinations on the system were evaluated separately in internal and external frames. Especially in elastic design and force-based designs, the effect of this coefficient has been evaluated in buildings with different coefficients in this study. As an example, the number of floors of the studied buildings were modeled as 8, 10, 13 and 15-storey composite moment-resisting frames. During the modeling, the sensitivity coefficient was evaluated to be $0<\theta\leq0.1$ and $0.1<\theta\leq0.2$ in two different intervals. In the evaluations, Nonlinear Time History analyzes, and nonlinear element and material models were used to evaluate the nonlinear behavior. To evaluate the behavior of the systems, the average and maximum values of the interstory drift ratios were carried out. In systems consisting of exemplary composite moment-resisting frames, it has been theoretically evaluated that there were important effects of the use of this coefficient, especially in outer frames.

1 Dr. Ögr. Üyesi, Munzur University, Dep. of Emergency Aid and Disaster Management, serkanetli@munzur.edu.tr, Orcid: 0000-0003-3093-4106

2 Ögr. Gör. Dr. Munzur University, Tunceli Vocational Schools, melekakgul@munzur.edu.tr, Orcid: 0000-0001-8815-3762

https://doi.org/10.58830/ozgur.pub130.c604

1. Introduction

Composite structures designed by combining the superior properties of steel and concrete together provide effective solutions to the designer during the design stage. CMRFs can be characterized as one of the most economical designs in terms of structural behavior and strength characteristics, when system features and element capacities are considered. The economy required in this manner is especially important in buildings with a service life in areas that are likely to be affected by severe earthquakes. During the engineering design of composite structures for earthquake effects, the high ductility that steel and concrete will show as expected on the basis of working together on demand increases the theoretical and practical applicability of the structure in the face of high energy formation that will result from repeated earthquake loads. For these structures, which are suitable to be designed as moment-bearing frames (MRF), the lateral dynamic loads that constitute the main effect in earthquake forces are mainly met by the flexural strength capacities of beam and column elements. In this case, the biggest challenge during the design of such structures is the design of the column elements as composite elements. When the methods of capacity design principles are applied under earthquake effects, ductility should be the first determining factor for the designer in terms of engineering (Elghazouli et al., 2008). When the previous studies in the literature related to the composite structures are examined, several studies have been done to examine the parameters related to the connection points (Hawkins & Mitchell, 1984; Leon et al., 1998), shear interaction (Caldara, 1998), floor effect (Plumier, 2000) and seismic performance (Miranda, 2012; Thermou et al., 2004). Moreover, in the previous studies by Denavit et al., the behavior of CFST elements was examined in detail and the behavior of the structures of CMRFs systems consisting of these elements was evaluated. Especially after this condition, which is an important parameter in the calculation of design loads, is met, ductility, which is the design criterion of the structures planned to be designed, is provided by the composite columns designed in relation to the behavior of CMRFs according to the design requirements. Achieving the goal of proper building design is not always sufficient with simple techniques used in calculations involving traditional design methods. On the other hand, it is very important to detail the behavior of the building elements closest to reality, which will occur with the effect of the forces they will be exposed to during an earthquake, in the design. The behavior of the building elements against these dynamic effects is addressed to the building systems in accordance with the behavior factors specified by the design codes. These factors, which are included in force-based designs, which is

one of the traditional design styles, are the values used to reduce the lateral loads that will occur in the structure (under the effect of earthquake) with mathematical expressions during the calculation. The "q" behavior factors specified in European codes are used for this purpose. In addition, to reach the most sufficient or most accurate validity from these factors in designs, it is very related to the system features to be designed and the accuracy of the basic assumptions of the elements in the system. More importantly, considering the region where the structure will be built, it should not be forgotten that the structural behavior of the structure under the influence of different dynamic loads can be quite transitory in the design of the structure, which also originates from the fundamental properties of the earthquake loads. (Broderick & Elnashai, 1996; Elghazouli et al., 2008). In many studies of the structures produced in this type and the structures produced in the relevant national standards, similar properties are evaluated in the relevant designs (Etli, 2021, 2022; Etli & Güneyisi, 2020, 2021, 2022b, 2022a; Güneyisi & Etli, 2020).

In this study, CMRFs were analyzed using nonlinear dynamic analysis (NDA) technique with time-history records (TH) in different properties. CMRFs were designed as 8-,10-,13- and 15-story according to the Eurocode seismic design specifications. Moreover, in the seismic design stage, only θ parameter properties were selected in different range as $0<\theta\leq0.1$ and $0.1<\theta\leq0.2$. Therefore, in the seismic design situation there are two cases, the first one is for $0<\theta\leq0.1$ and second one is $0.1<\theta\leq0.2$. Then, the CMRFs were divided in two frames according to the position, the frames were selected as inner and outer frames. Finally, in the study there were four case and they classified as Case-I is inner frame for $0<\theta<0.1$, Case-II is inner frame for $0.1<\theta\leq0.2$, Case-III is outer frame for $0<\theta\leq0.1$ and Case-IV is outer frame for $0.1<\theta\leq0.2$.

In seismic design stage of all CMRFs, the CMRF were modelled as elastic elements according to the Eurocode. Then, in the NDA stage of CMRFs, the CMRFs members were remodeled using distributed plasticity force-based elements. The NDAs were performed with TH and TH records were selected in 3 different groups. The groups were created using FEMA earthquake record classification. Moreover, the earthquake acceleration was selected based on the seismic design stage spectra parameters. The parameters of elastic design spectra were selected as Ground-C class and the earthquake magnitude is greater than 6.5. Then, the TH records groups and specifications are selected as far-field (FF), near-field without-pulse (NF-NP) and near field with pulse (NF-P) from FEMA guidelines. Each TH record

groups contained 10 TH records. After selection of TH records according to the given above specifications, TH record were scaled for seismic design elastic spectra using the Seismomatch software. After that point, the CMRFs were analyzed using NDA method with FF, NF-NP, and NF-P type TH records. The results of NDAs were evaluated in terms of interstory drift ratio (IDR), roof drift ratio (RDR), base-shear coefficient, base moment, roof accelerations. The results are presented at the next session.

2. Structural Configuration and Design Procedures

8, 10, 13 and 15-story CMRFs were used for the comparison of the seismic behavior. Regarding the designs of the structures in the study, earthquake resistant structures were designed with Eurocode-8 (EN 1998-1, 2004) by using the earthquake spectra obtained with 0.2g peak ground acceleration (PGA) in these structures whose specific parameters were examined after design. In the CMRF multi-storey structures designed, the designs were carried out with multiple compartments and the plan geometries of all structures were ensured to be the same. The selected plan and the system facade views of the designed buildings are presented in Figure 1. The CFST columns were placed every 7 m in the x-direction and y-direction to maintain the system symmetry. Considering the rigid diaphragm formation in the floors, the deformations under vertical loads and the ductility capacity of the beams, the floor thicknesses were dimensioned by considering the design features given in the relevant design codes. Hollow square section steel box profiles (SHS) selected from the catalogs published by European steel manufacturers in composite column elements planned to be used in CFSTs due to earthquake resistant design, and sections of steel beams to be used in composite beams were selected. The analyzes continued with the assumption that there is a complete shear interaction between the steel beam and the concrete slab at the design stage in the design and strength properties of the composite beams within the system. During the earthquake resistant design of the building, a value of 2 kN/m^2 was chosen for the dead load in the pavement and spatial partitions in addition to the dead load and slab weight transferred from the floors. The live load on the floor is used as 3 kN/m^2 in the calculations. As a result of the analyzes made on the system under the gravitational loads, the structural elements with sufficient strength in section properties were selected, and the CMRFs were evaluated in terms of earthquake resistant designs.

Fig. 1. Structural arrangement for the 5, 10, 15 and 20 story modelled structures: (a) Plan configuration and (b) Elevation of moment-resisting frame

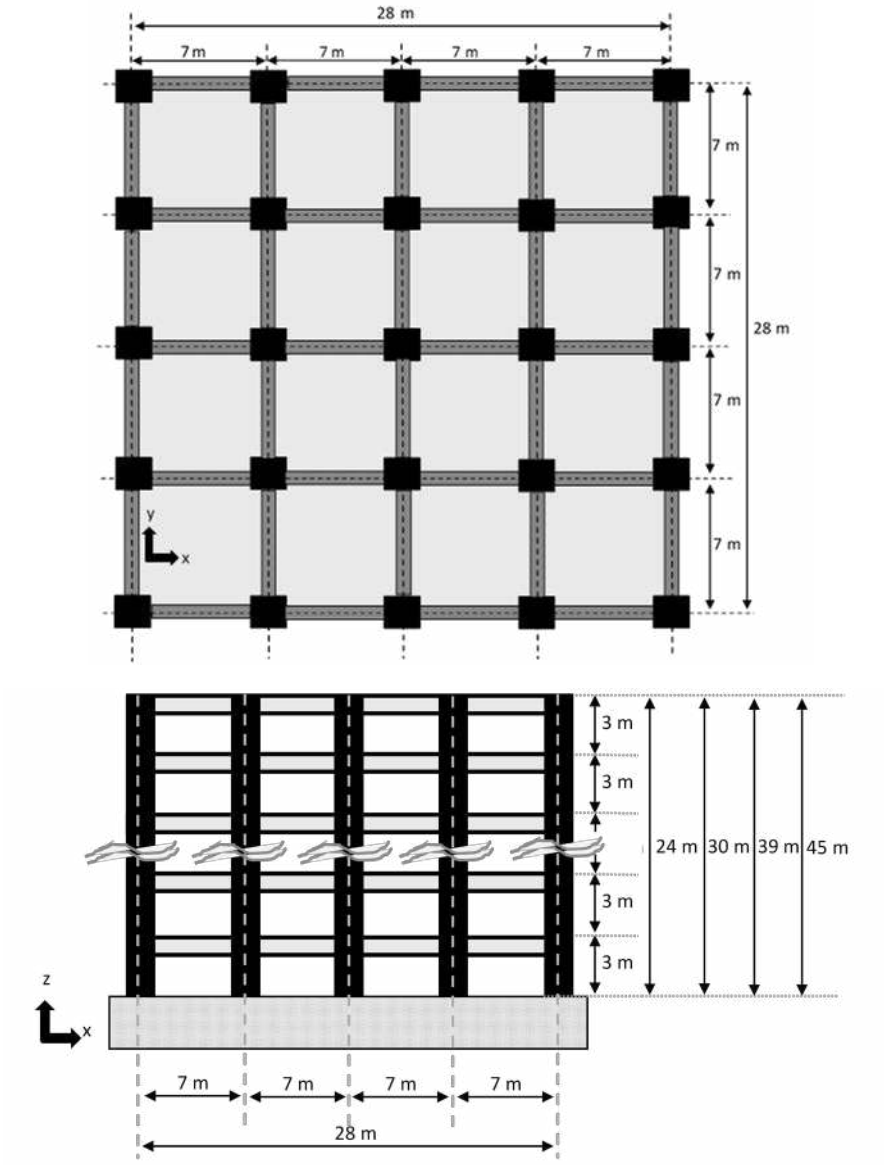

Considering the Eurocode-8 (EN 1998-1, 2004) conditions in the design of the structures, high ductility (DCH) systems were selected. Response spectra are used to calculate the forces transmitted from the ground to the structure due to the earthquake effect. There are some data needs in

the formulas included in the recommendations of the standards for these response spectra. In addition to the PGA values selected in the design of the structures that are subject to evaluation in the study, the C class soil was evaluated as the soil type characteristic of the place where the structure will be built. On the other hand, Eurocode-8 (EN 1998-1, 2004) is also included in a classification of seismicity, that is, the magnitude f-value of the earthquake. By paying attention to these situations, type-1 spectrum calculations were used, considering the seismicity of the location where the construction activities will be carried out. When the system properties are evaluated in earthquake resistant structural design for Eurocode-8 (EN 1998-1, 2004), it is considered appropriate to use the modal analysis method in these structures. In addition, as is known, the section designs that are not made in accordance with the selected structural behavior coefficient may cause the structures not to reach the selected ductility value. Therefore, the guidelines for the relevant ductility conditions for Eurocode-8 (EN 1998-1, 2004) have been considered, and attention has been paid to the suitability of element sections and behaviors. For multi-span and multi-storey buildings, 5□u/□1 formula is used in the calculation of the proposed behavior factor in Eurocode-8 (EN 1998-1, 2004). As a result, the behavior factor is obtained with the mentioned values as 6.5. On the other hand, it has been reported in previous studies that wind pressure does not have a significant effect during element sizing in such structural elements (Acun, 2012).

During the earthquake resistant design of the building, the necessary features for the strength capacities of the elements as well as the drift ratio between the floors and thus the limit values for the stability of the structure were taken into consideration. After calculating the earthquake forces, the sensitivity coefficient defined in Eurocode-8 (EN 1998-1, 2004) was used to reflect the second-order effects and the effects of these effects on the elements in the design. Economic designs were tried to be used by converging to the minimum cross-section capacities by using two different group designs, with the value of the coefficient taken as the basis in the CMRFs designs between 0-0.1 and 0-0.2. The calculation method required for the aforementioned sensitivity coefficient "θ" is as follows:

$$\theta = \frac{P_{tot} \times d_r}{V_{tot} \times h} \quad (1)$$

Among the parameters in the equation, the cumulative gravity load for P_{tot} and the total earthquake shear force acting on the ground level to the building foundation for V_{tot} are included in the calculations. The story heights and the values of the offsets of the floors calculated during the design

are symbolized as h and d_r, respectively. The design shift value, which is considered as the limit value during design, is obtained by multiplying the elastic relative drift and the behavior factor. Another inequality in Eurocode-8 (EN 1998-1, 2004) is given as follows for the evaluation of the story drifts of the building after calculating the lateral seismic forces:

$$d_r \times \nu \leq \psi \times h \tag{2}$$

It is stated that the definition made in the standard for the ψ value in the inequality given above is used to reflect the behavior of the non-structural elements of the building design. Regarding this value, the values given in Eurocode-8 (EN 1998-1, 2004) are 0.5%, 0.75% and 1.0%. While choosing these values, it is stated that they are used in structural systems designed with brittle, ductile and non-structural or insulated elements, respectively. The integration of the characteristic properties determined in the service properties and the inter-floor drift properties to this limit state is given as the value of ν, this value is between 0.4 and 0.5. While the ψ value was used as 0.75% for the design of the structures designed within the scope of this article, the ν value was chosen as 0.5.

It has been stated that the second-order effects, which are controlled by the definition of the sensitivity coefficient and symbolized by θ, reach up to 0.2 within the scope of the study for some case studies. Therefore, after the θ value exceeds 0.1, it should be considered during the seismic design with the help of a simplified formula given in Eurocode-8 (EN 1998-1, 2004). This simple formula is considered by multiplying the calculated seismic effects at the floor level by the factor calculated by 1/(1-θ) to be included in the calculations for the second order effects.

For a design constructed with weak beam/strong column behavior, the special rule used during the design of composite columns in moment-transmitting frames after the ductile behavior of beams is provided by section designs is given below:

$$M_{Ed} = M_{Ed,G} + 1.1 \times \gamma_{ov} \times \Omega \times M_{Ed,E} \tag{3}$$

In the given formula, the moment values for $M_{Ed,G}$ and $M_{Ed,E}$ are given as calculated after gravity and seismic analysis, respectively. In addition, γ_{ov} value was defined to reflect the material properties and this value was included in the calculations as 1.25 within the scope of the study. Another term Ω value in the expression is calculated as the beam overload factor, which is calculated with the ratio $M_{pl,Rd,i}/M_{Ed,i}$ and selected to be the smallest

of the values. The values in the ratio are considered in the calculations as the plastic moment capacity and the design moment value of the "ith" beam, respectively.

Moment frame systems are since the bearing capacities of the vertical carrier columns are stronger than the beams. Reaching the shear capacities of concrete beams after bending capacities and trying to provide buckling formation in steel braces before the columns are basically three important examples of capacity design. Another general rule used in all frame structure types in Eurocode-8 (EN 1998-1, 2004) is that the moment strengths of all columns on a certain joint point must be at least 1.3 percent of the moment strengths of the beams. This requirement is formulated as follows:

$$\sum M_{Rc} \geq 1.3 \times \sum M_{Rb} \quad (4)$$

$\sum M_{Rc}$ and $\sum M_{Rb}$ in the given formula are expressed as the total moment capacity of columns and beams at the same joint, respectively.

For all designed CMRFs, the design analysis is two-step. The first is the design under gravity loads for the availability limit state (SLS), which is defined as preliminary analysis. In all designed CMRFs, the maximum bearing capacity (ULS) design criteria for the seismic ultimate limit state given in Eurocode-8 (EN 1998-1, 2004) were checked after the SLS design for an earthquake effect of 0.2g. Ensuring ULS and SLS status is essential. To obtain the desired and modeled behavior during earthquake resistant design in CMRF models, CFST columns are welded and rigidly connected with steel beams at the nodal (Elghazouli et al., 2008).

Table 1. Modal periods and mass ratios of the analyzed frames

	T_1 (s)	T_2 (s)	T_3 (s)	U_1 (%)	U_2 (%)	U_3 (%)	T (s)
8stry-I	1.081	0.336	0.179	79.258	10.400	4.394	1.146
10stry-I	1.181	0.372	0.202	78.911	10.134	4.186	1.254
13stry-I	1.364	0.436	0.241	78.762	9.970	3.910	1.452
15stry-I	1.467	0.467	0.258	78.171	10.030	3.909	1.561
8stry-II	1.344	0.404	0.206	77.749	10.917	4.811	1.419
10stry-II	1.650	0.500	0.257	77.036	10.690	4.699	1.744
13stry-II	1.886	0.583	0.309	77.140	10.276	4.341	1.998
15stry-II	2.118	0.649	0.340	76.347	10.372	4.421	2.242

Table 2. Member properties of the structure

	Beam	Column	Concrete	Steel
8stry-I	IPE 500	550X40	C30	S275
10stry-I	IPE 550	600X50		
13stry-I	IPE 600	650X60		
15stry-I	HEA 550	750X60		
8stry-II	IPE 400	550X40		
10stry-II	IPE 400	600X45		
13stry-II	IPE 450	650X60		
15stry-II	IPE 450	750X60		

Modal periods and mass ratios of the analyzed frames were presented in Table 1. In the seismic design of CMRFs, natural vibration periods of CMRFs were change according to the selected θ values in the seismic design stage. According to the θ value range, CMRFs structures names were given with 8stry-I, 10stry-I, 13stry-I and 15stry-I for $0<\theta\leq0.1$ and 8stry-II, 10stry-II, 13stry-II and 15stry-II for $0.1<\theta\leq0.2$. Modal periods of 8stry-I, 10stry-I, 13stry-I and 15stry-I structures are greater than the modal periods of 8stry-II, 10stry-II, 13stry-II and 15stry-II, respectively. CMRFs structures has greater member section for the $0<\theta\leq0.1$ case than in the case of $0.1<\theta\leq0.2$ situation whereas composite members section smaller in the case of $0.1<\theta\leq0.2$ (Table 2). Therefore, CMRFs stiffness decreases in the case of $0.1<\theta\leq0.2$ situation against the $0<\theta\leq0.1$ case, so that the periods of the $0.1<\theta\leq0.2$ case CMRFs are higher periods.

Table 3. Design properties of the analyzed frames

	W_{FRAME} (kN)	V_{tot}	d_r	θ	α
8stry-I	17561.3	974.71	0.0184	0.0920	5.2231
10stry-I	22374.2	1337.03	0.0192	0.0912	6.3596
13stry-I	29765.9	1551.90	0.0173	0.0962	7.1942
15stry-I	35633.8	1729.22	0.0162	0.0957	8.6876
8stry-II	17488.8	922.08	0.0267	0.1400	7.4944
10stry-II	22150.3	966.50	0.0265	0.1726	9.9061
13stry-II	29534.2	1144.14	0.0239	0.1766	11.8225
15stry-II	35307.1	1203.10	0.0228	0.1929	16.6806

Some parameters were calculated at the design stage is presented in Table 3. These parameters were given with W_{FRAME}, V_{tot}, d_r, θ and α, these parameters defined as structure weight, earthquake shear force acting on the floor level, design drifts, sensitivity coefficient and the over-strength of column against the beams. It can be clearly seen from Table 3 that V_{tot} values of CMRFs for in the case of $0<\theta\leq0.1$ greater than in the case of $0.1<\theta\leq0.2$ ones. Similarly, 8stry-I, 10stry-I, 13stry-I and 15stry-I structures d_r and α values are greater than the 8stry-II, 10stry-II, 13stry-II and 15stry-II structures, respectively. This is mainly provided the CMRFs stiffness. Moreover, the section size of beams is greater size in the 8stry-II, 10stry-II, 13stry-II and 15stry-II structures, while the column size was similar.

3. Details of numerical modelling

In this section, the properties related to the steel and concrete models selected in order to obtain a realistic behavior in non-linear analyzes of the composite beams in which the steel beams working with the column and slab obtained by using CFST sections are explained. While the structures designed to be earthquake resistant and inspected by the provisions of Eurocode-8 (EN 1998-1, 2004) are examined under earthquake forces, the behavior of concrete in structural elements due to earthquakes in the model is evaluated by using the model developed by Martinez-Rueda and Elnashai (Martínez-Rueda & Elnashai, 1997) as the concrete model. considered. Regarding this concrete material model, it was defined as "con_ma" in the Seismostruct software and the sample image of the model taken from the software is presented in Figure 2(a). In the "con_ma" model included in the software, while the effects of the confinement effect occurring around the concrete or reinforced concrete were determined, the related effect was used in the "con_ma" model thanks to the coefficient obtained by simulating the circular spiral reinforcement. Moreover, in the studies, it is seen that the data obtained in the experimental and theoretical studies with concrete filled tubes are higher than the concrete elements surrounded by circular reinforcements (Choi & Xiao, 2010; Uy, 2001; Xiao & Wu, 2000). Since the structures were not examined under the influence of earthquake records after the earthquake resistant structural design, the confinement effect that will occur in the concrete in the CFST columns is provided by the steel SHS section used in the outermost part of the element section. The evaluation of the winding effect is defined using the kc value in the selected concrete model of the Seismostruct (Seismosoft, 2016) software. The confinement factor value kc is defined by the ratio between the compressive strength of the coiled concrete model and the concrete strength obtained by the

confinement effect. Susantha et al. (Susantha et al., 2001) created some theoretical calculation methods for determining the load capacities of such cross-section members, namely CFST members. When the data obtained from the calculations and models produced using theoretical calculations and the data obtained from the experimental models are compared, it has been shown that the necessary convergence has occurred. Susantha et al. (Susantha et al., 2001) used experimental work on a large number of CFST elements (with different geometry and other mechanical parameters) and theorized calculations. The physical and mechanical properties of the CFST composite column used in the design models obtained are similar or close to the cross-section properties of the element used in previous studies in the literature (Etli, 2021, 2022; Etli & Güneyisi, 2020, 2021, 2022b, 2022a; Güneyisi & Etli, 2020).

For the material behavior of the sections consisting of steel profiles in composite beams, information on material models operating under the effect of elasto-plastic cyclic loads is used in material modeling. This model is defined as "stl_mn" in Seismostruct software and the software image of the model is given in Figure 2(b). It is frequently used in the literature as a material behavior model of steel developed by researchers by examining experimentally and theoretically by various researchers (Antoniou et al., 2008; Filippou et al., 1983; G. Monti, C. Nuti, 1996; Menegotto & Pinto, 1973; Shahrooz et al., 1993). On the other hand, there is a need for element modeling including material models. In the definitions of element behavior, many force and displacement-based models are mentioned in the literature. Some modeling techniques are given as defined in the Seismostruct (Seismosoft, 2016) software, it is known that in these element modeling techniques, the models of the elements created using steel and concrete models, show sufficient convergence to the previous experimental results in the literature when the sections are modeled with fiber elements (Xu et al., 2018). Experimental data of test samples used in the literature for CFST (Baba et al., 1995; Huang et al., 2018; Srinivasan & Schneider, 1999; Tomii et al., 1977), and material models described above, and many modeled elements using fiber were examined by researchers (Etli, 2021, 2022; Etli & Güneyisi, 2020, 2021, 2022b, 2022a; Güneyisi & Etli, 2020). It is stated that the results of these models, which are examined with the section model in the Seismostruct (Seismosoft, 2016) software, are obtained converging to the experimental test results (Boukhalkhal et al., 2019; Bruneau et al., 2008; Li et al., 2018; Xu et al., 2018; Zhang & Gao, 2019).

Fig. 2. a) Concrete model and b) steel model schematic view from Seismostrucrt software (Seismosoft, 2016)

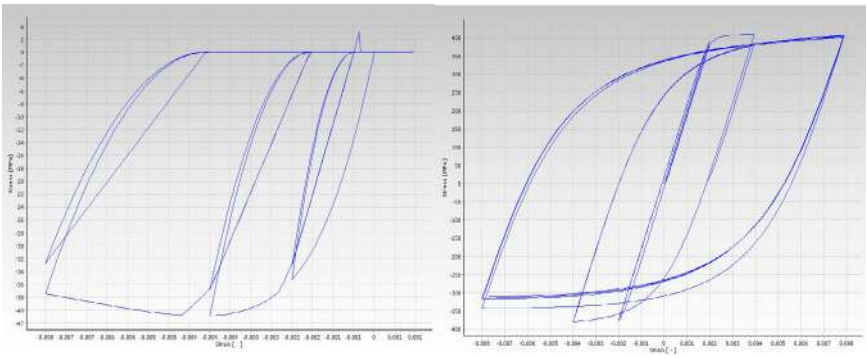

(a) (b)

The models developed for the region, which is defined as the junction region, have been previously investigated experimentally and theoretically by researchers in the literature for the junction points of structural steel elements (e.g., (Kim & Engelhardt, 2002)), reinforced concrete joints (e.g. (Altoontash, 2004)) and junction points of composite elements (e.g., (Fukumoto & Morita, 2005; Kanatani et al., 1987; Muhummud, 2003)). The port properties of the modified Richard-Abbott Model are included to simulate the behavior by defining parameters within the Seismostruct software. The behavior related to this joint point has been programmed by Nogueiro et al. (Nogueiro et al., 2005) and it is possible to simulate any possible steel and composite connection in practice (e.g. welded-flange bolted-web connection, extended end-plate connection, flush end-plate connection, angle connection, etc.). In the study, CFST elements and composite beams are modeled using the Modified Richard-Abbott Model to consider the joints in the behavior.

Seismostruct (Seismosoft, 2016) software was used for nonlinear analysis of CMRFs consisting of composite columns and beam sections modeled using fiber section elements. During the analysis, models were used for composite beams as a complete shear connection between the steel beam body and the concrete slab (Castro, 2006). Another parameter used in beams, 1.225 m, is reflected in the calculations as the effective floor width for inner frame and also 0.6125 m were used at outer frames. In a study in the literature, Miguel, and Castro (Castro, 2006), Eurocode-4 (EN 1994-1-1, 2004) and Eurocode-8 (EN 1998-1, 2004) calculated the effective slab width calculation models. compared. They reported that the models

of the obtained theoretical data helped to obtain the experimental behavior with sufficient accuracy. In another study, Castro et al. (Castro et al., 2007) produced test samples related to the effective slab widths used in composite beams and presented that their experimental results converged with those suggested in such codes.

Steel elasticity modulus (E), poisson ratio (υ) and hardening coefficient (μ) values of the materials used in element models were taken as 210 × 10^3 N/mm^2, 0.3 and 0.5%, respectively. The cross-sectional properties of the elements used in the design and the classes of materials used in these elements are given in Table 2. To summarize these properties, the yield strength of the structural steels used is S275 and the concrete class used in all these buildings is considered as C30 (Etli, 2021, 2022; Etli & Güneyisi, 2020, 2021, 2022b, 2022a; Güneyisi & Etli, 2020).

A schematic representation of the modeling of the cross sections of the composite elements of CMRF structures with the fiber elements in the Seismostruct (Seismosoft, 2016) software is given in Figure 3. In addition, these elements are modeled by the "infrmFB", which is defined as the inelastic force-based frame element in the Seismostruct software. Columns and beams designed as composite members are divided into 5 elements.

Fig. 3. Fiberized sections view for (a) CFST columns' sections, (b) composite beam section.

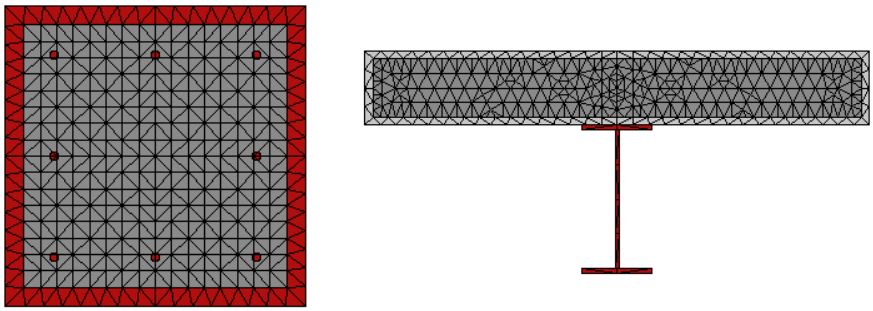

(a) (b)

Fig. 4. Model views from SeismoStruct software.

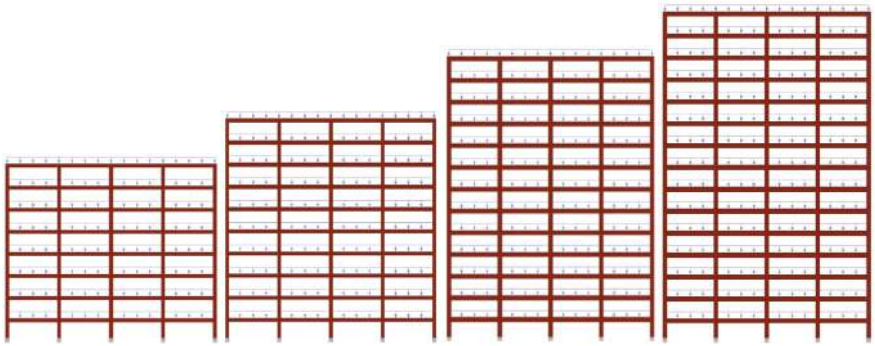

TH records properties given for NDAs of CMRs were given in Table 4. It can be clearly seen that the records properties were properly selected according to the elastic seismic design spectra. The parameters of V_{s30} and M are the preliminary determination properties for selection and these parameters of V_{s30} were defined as the average seismic shear-wave velocity from the surface to a depth of 30 meters while the M is the magnitude of TH record.

Table 4. Details of earthquake records

No.	Record Seq. No.	Component	M	Year	Name	Vs_{30} (m/sec)	Source (Fault Type)	Rjb (km)	Rrup (km)	PGA max (g)	PGV max (cm/s.)
Far-Field Earthquake Record Set											
TH-1	125	0	6.5	1976	Friuli, Italy	425	Thrust	14.97	15.82	0.357	22.8
TH-2		270								0.315	30.5
TH-3	1111	0	6.9	1995	Kobe, Japan	609	Strike-slip	7.08	7.08	0.483	46.8
TH-4		90								0.464	38.3
TH-5	1148	0	7.5	1999	Kocaeli, Turkey	523	Strike-slip	10.56	13.49	0.210	14.0
TH-6		90								0.134	40.1
TH-7	1485	E	7.6	1999	Chi-Chi, Taiwan	705	Thrust	26.00	26.00	0.473	50.1
TH-8		N								0.507	46.4

Table 4. Details of earthquake records (continued)

No.	Record Seq. No.	Component	M	Year	Name	Vs_{30} (m/sec)	Source (Fault Type)	Rjb (km)	Rrup (km)	PGA max (g)	PGV max (cm/s.)
TH-9	1633	L	7.4	1990	Manjil, Iran	724	Strike-slip	12.55	12.55	0.515	42.5
TH-10		T								0.497	50.6
Near-Field Earthquake Record Set											
Pulse Records Subset											
TH-11	802	0	6.9	1989	Loma Prieta	371	Strike-slip	7.58	8.50	0.514	41.6
TH-12		90								0.326	46.0
TH-13	828	0	7	1992	Cape Mendocino	713	Thrust	0.00	8.18	0.591	49.3
TH-14		90								0.662	88.5
TH-15	879	260	7.3	1992	Landers	685	Strike-slip	2.19	2.19	0.725	133.4
TH-16		345								0.789	28.1
TH-17	1086	90	6.7	1994	Northridge-01	441	Thrust	1.74	5.30	0.605	77.5
TH-18		360								0.843	129.4
TH-19	1529	E	7.6	1999	Chi-Chi, Taiwan	714	Thrust	1.49	1.49	0.304	91.7
TH-20		N								0.172	66.4
No Pulse Records Subset											
TH-21	126	0	6.8	1976	Gazli, USSR	660	Thrust	3.92	5.46	0.702	66.2
TH-22		90								0.864	67.7
TH-23	825	0	7	1992	Cape Mendocino	514	Thrust	3.85	10.72	1.494	122.3
TH-24		90								1.039	42.4
TH-25	1004	270	6.7	1994	Northridge-01	380	Thrust	0.16	3.85	0.753	77.7
TH-26		360								0.932	76.3
TH-27	741	0	6.9	1989	Loma Prieta	376	Strike-slip	0.00	6.96	0.645	56.0
TH-28		90								0.483	47.6
TH-29	753	0	6.9	1989	Loma Prieta	462	Strike-slip	0.00	8.44	0.456	51.4
TH-30		90								0.502	44.5

Table 5. Details of earthquake records after scaling

No.	PGA_{max} (g)	PGV_{max} (cm/s.)	PGA/PGV	Arias Intensity: (m/sec)
Far-Field Earthquake Record Set				
TH-1	0.273	33.8	0.0081	0.757
TH-2	0.246	29.7	0.0083	0.772
TH-3	0.229	22.5	0.0102	1.339
TH-4	0.240	20.8	0.0115	1.056
TH-5	0.257	27.5	0.0093	1.034
TH-6	0.281	57.4	0.0049	1.104
TH-7	0.323	33.3	0.0097	0.973
TH-8	0.374	33.2	0.0112	0.732
TH-9	0.255	33.0	0.0077	1.160
TH-10	0.232	26.3	0.0088	1.332
Near-Field Earthquake Record Set				
No Pulse Records Subset				
TH-11	0.222	25.9	0.0086	0.654
TH-12	0.224	30.7	0.0073	0.741
TH-13	0.211	27.2	0.0078	1.104
TH-14	0.232	29.1	0.0080	1.239
TH-15	0.304	25.7	0.0118	0.858
TH-16	0.232	23.2	0.0100	0.928
TH-17	0.360	39.3	0.0092	0.484
TH-18	0.358	33.3	0.0108	0.559
TH-19	0.343	30.4	0.0113	0.637
TH-20	0.303	19.2	0.0157	0.946
Pulse Records Subset				
TH-21	0.305	31.7	0.0096	0.635
TH-22	0.252	40.9	0.0062	0.842
TH-23	0.268	21.6	0.0124	1.148
TH-24	0.271	35.6	0.0076	0.753
TH-25	0.278	41.1	0.0068	0.963
TH-26	0.227	29.1	0.0078	0.858
TH-27	0.289	31.2	0.0093	0.966
TH-28	0.235	39.5	0.0059	0.548
TH-29	0.238	52.7	0.0045	1.329
TH-30	0.260	49.9	0.0052	1.630

4. Behavior of example structures

The structural behaviors were compared with the IDR (inter-story drift ratio). IDR were accepted as a critical design and performance factor in the literature. The comparation of structures were presented below.

4.1. Behavior of example structures inner frames

For each record in Figure 5 and Figure 6, IDR_{max} and IDR_{ave} values of the analyzes performed in Case-I and Case-II CMRFs are given. In Figure 4, IDR_{max} values obtained because of NDAs made using the FF, NF-NP, and NF-P type THs of Case-I and Case-II buildings are presented comparatively. In this stage of this work, the IDR_{max} value of structure were investigated under three different type of TH record as FF, NF-NP and NF-P type of strong ground motion as mentioned above. In this part, the same CMRFs were divided in three sections in terms TH records used in NDAs, firstly the IDR_{max} values were examined with FF type TH, then it's examined with NF-NP type TH record and finally it's investigated with NF-P type TH records. At the first stage of NDAs, the IDR_{max} values of Case-I structures with 8-, 10-, 13- and 15-story CMRFs were 21.74% (TH-8, Chi-Chi, Taiwan), 30.77% (TH-9, Manjil, Iran), 18.81% (TH-6, Kocaeli, Turkey), and 6.41% (TH-5, Kocaeli, Turkey) smaller than the IDR_{max} values of Case-II structure, respectively. In second stage of NDAs, the IDR_{max} values of Case-I structures with 8-, 10-, 13- and 15-story CMRFs were 25.68% (TH-18, Loma Prieta), 28.9% (TH-12, Gazli, USSR), 33.2% (TH-19, Loma Prieta), and 23.53% (TH-14, Cape Mendocino) smaller than the IDR_{max} values of Case-II structure, respectively. Finally, the last stage for NDAs, the IDR_{max} values of Case-I structures with 8-, 10-, 13- and 15-story CMRFs were 24.68% (TH-22, Loma Prieta), 53.57% (TH-28, Northridge-01), 11.01% (TH-29, Chi-Chi, Taiwan), and 7.2% (TH-29, Chi-Chi, Taiwan) smaller than the IDR_{max} values of Case-II structure, respectively. The maximum desired level of damage to a structure under specific earthquake design level is expressed as performance level. Based on FEMA-273 (FEMA 273, 1997) (1997) and Vision 2000 ("Vision 2000, Conceptual Framework for Performance Based Seismic Engineering of Buildings.," 1995) (1995), the performance level can be divided into seven performance stages which include fully operational, operational, immediate occupancy, damage control, life safety, collapse prevention and near collapse. The drifts proposed for these performance levels are 0.2% for fully operational (FO), 0.5% for operational (OP), 1% for immediate occupancy (IO), 1.5% for damage control (DC), 2% for life safety (LS), and 2.5% for collapse prevention (CP), and 3% for near

collapse (NC). In this way, when the Case-I and Case-II structures were examined in three group type of TH records, the 8-story CMRFs inside both group structure were reached the IO performance level in the first and final NDAs stage were examined. Moreover, according to the IDR_{max} value of the 15-story CMRFs structures, it is the only structure stayed under the IO performance level between the Case-II structures for FF and NF-P type TH records. On the other hand, only the 10-story CMRF reached to the IO performance level for NF-NP type records, and it is the only structure between the Case-I CMRFs structure reached only this performance level.

Variation of IDR_{ave} with the story for each earthquake group is given in the Figure 6. When the IDR_{ave} values of Case-I structures are examined for NDAs with FF type records, the IDR_{ave} values remain between 0.0075 and 0.0093. In NF-NP type NDAs records results, the IDR_{ave} values of Case-I structures are examined, IDR_{ave} values remain between 0.0075 and 0.0093 as same as FF type records NDAs results. Final part of records NF-P types of NDAs results, the IDR_{ave} values of Case-I structures are examined, the IDR_{ave} values remain between 0.0075 and 0.0098. The IDR_{ave} values of the Case-II structures are examined, the IDR_{ave} values remain between 0.0086 and 0.012 for FF type TH records of NDAs, and between 0.0086 and 0.011 for NF-NP type TH records of NDAs. Moreover, for NF-P type TH records of NDAs, the IDR_{ave} values stay between 0.0088 and 0.012 (Figure 6).

Fig. 5 Variation of IDR_{ave} with the story for each earthquake group according to sensitivity coefficient (θ) change in inner frames

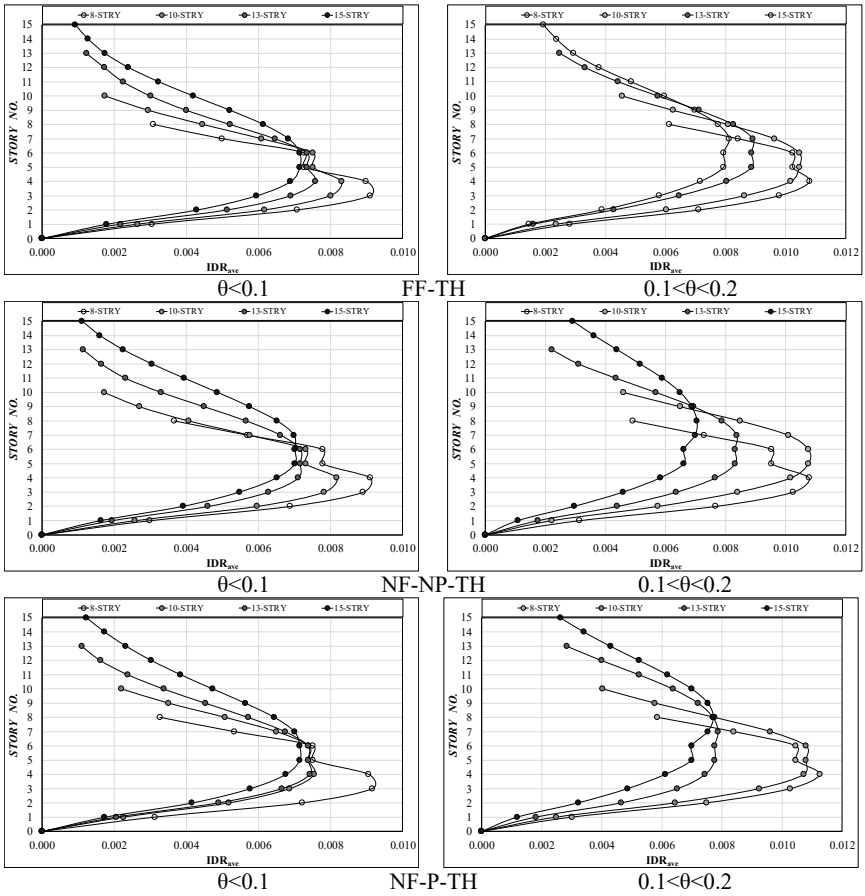

Fig. 6 Variation of the IDR_{max} for each earthquake group according to sensitivity coefficient (θ) change in inner frames

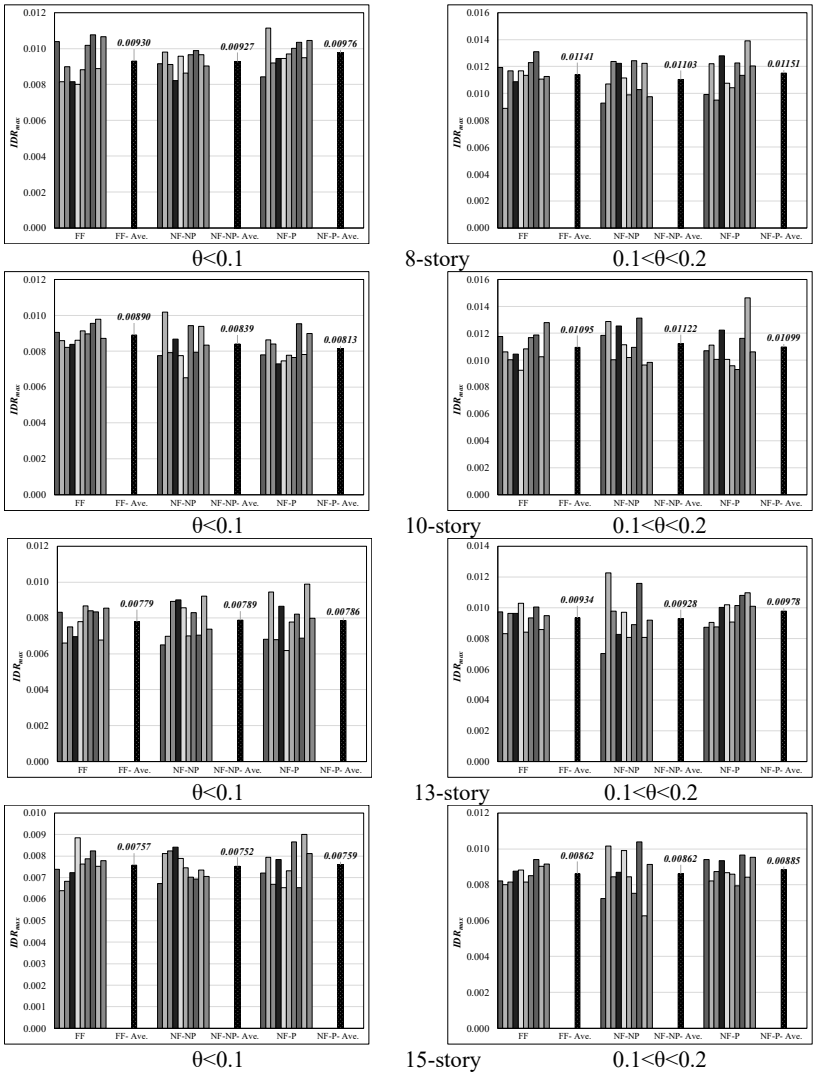

4.2. Behavior of example structures outer frames

In Figure 7 and Figure 8, the IDR_{max} and IDR_{ave} values of Case-III and Case-IV CMRFs were given for each record and also each groups average. When the Case-III structures NDAs were evaluated for FF type TH records, the IDR_{max} values were obtained as 0.00879 (TH-4, Kobe (Japan)), 0.00803 (TH-6, Kocaeli (Turkey)), 0.00710 (TH-3, Kobe (Japan)) and 0.00758 (TH-9, Manjil, (Iran)) for 8-,10-,13- and 15-story CMRFs, respectively.

Moreover, these IDR_{max} values were obtained smaller than the IDR_{max} values of Case-I structures NDAs evaluated for FF type TH records. These TH records were observed differently for each 8-, 10-, 13- and 15-story structure in Case-I and Case-III structures. On the other hand, when the Case-IV structures NDAs were evaluated for FF type TH records, the IDR_{max} values were obtained as 0.01079 (TH-3, Kobe, (Japan)), 0.01120 (TH-8 (Chi-Chi, Taiwan), 0.01062 (TH-10, (Manjil, Iran)), and 0.00958 (TH-10, (Manjil, Iran)) for 8-,10-,13- and 15-story CMRFs, respectively. Case-III structure IDR_{max} values smaller than Case-IV structure IDR_{max} values for NDAs made with FF type TH records, the difference is 22.8%, 39.6%, 49.5%, and 26.3% for 8, 10, 13 and 15-story CMRFs, respectively. TH-10 (Manjil, Iran) record were caused IDR_{max} values for 13- and 15-story CMRF both of the Case-IV structures. Moreover, Case-III and Case-IV structures IDR_{max} values shows different trends. Case-III structures shows decrease until 15-story structures but Case-IV structures IDR_{max} values increase at 10-story structure than it decreases continuously. The effective main earthquake record is similarly the effective component of earthquake records were changing with the structural seismic design parameters. Therefore, the component properties of earthquake records were investigated, and it was observed that the earthquake components where PGA/PGV (peak ground velocity) greater shows mostly biggest IDR_{max} values for 10-,13- and 15-story Case-III structures against the Case-IV structures (Table 5). For the NF-NP type TH records, the IDR_{max} values were obtained as 0.00898 (TH-20, Loma Prieta), 0.00880 (TH-11, Gazli, (USSR)), 0.00783 (TH-15, Northridge-01), and 0.00761 (TH-12, Gazli, USSR) for Case-III structures. For the fourth group with same TH records, Case-IV structures NDAs were evaluated, the IDR_{max} values were obtained as 0.01084 (TH-12, Gazli, USSR), 0.01182 (TH-13, Cape Mendocino), 0.00987 (TH-13, Cape Mendocino) and 0.00999 (TH-12, Gazli, USSR). Case-III structure has smaller IDR_{max} values than Case-IV structure for NDAs made with NF-NP type TH records, the difference is 20.8%, 34.3%, 26.1%, and 31.3% for 8, 10, 13 and 15-story CMRFs, respectively. In Case-III structures, the IDR_{max} results calculated for NF-NP type TH records shows almost a similar trend against the IDR_{max} results calculated for FF type TH records. In Case-IV structures, the IDR_{max} results calculated for NF-NP type TH records shows a different trend against the IDR_{max} results calculated for FF type TH records. The IDR_{max} results calculated for NF-NP type TH records were fluctuating and it reach the max value with 10-story structure then it decreases and then again it increase 15-story CMRFs in Case-IV structures. Like the results of the NF-NP group of IDR_{max}, the component properties

of the earthquake records were investigated, and it was observed that the earthquake components where PGA/PGV was higher showed the largest IDR_{max} values for each Case-III structure against the Case-IV structures (Table 5).

The last group of TH records is NF-P and the IDR_{max} values were obtained as 0.00878 (TH-30, Chi-Chi, Taiwan), 0.00836 (TH-27, Northridge-01), 0.00723 (TH-30, Chi-Chi, Taiwan), and 0.00736 (TH-22, Loma Prieta) for Case-III structures. On the other hand, when the Case-IV structures NDAs were evaluated for NF-P type TH records, 0.01092 (TH-30, Chi-Chi, (Taiwan)), 0.01202 (TH-29, Chi-Chi, (Taiwan)), 0.01088 (TH-29, Chi-Chi, (Taiwan)) and 0.01018 (TH-30, Chi-Chi, (Taiwan)). Case-III structure IDR_{max} values smaller than Case-IV structure IDR_{max} values for NDAs made with NF-P type TH records, the difference is 24.4%, 43.9%, 50.5%, and 38.4% for 8, 10, 13 and 15-story CMRFs, respectively. Moreover, when NDAs were evaluated for NF-P type TH records, it can be clearly seen that the dominant TH record is TH-29 and TH-30 (Chi-Chi, (Taiwan)) for both case and it has the lowest in terms of PGA/PGV values (Table 5).

When the Case-III and Case-IV structures were examined in three group type of TH records, the Case-III CMRFs inside group structure were stay under the IO performance level in all type TH records of NDAs. Moreover, Case-IV structures according to the IDR_{max} value of the NF-P type TH record of NDAs, all structures reached IO performance limit. However, Case-IV structures according to the IDR_{max} value of the FF type TH record of NDAs, all structures reached IO performance limit except 15-story CMRF. Case-IV structures according to the IDR_{max} value of the NF-NP type TH record of NDAs, almost all structures reached IO performance limit (just 13- and 15-story CMRF values 0.0099) (Figure 7).

IDR_{ave} variation with the story for each earthquake group is given in the Figure 8. When the IDR_{ave} values of Case-III structures are examined for NDAs with FF type records, the IDR_{ave} values remain between 0.0065 and 0.0081. In NF-NP type NDAs records results, the IDR_{ave} values of Case-III structures are examined, IDR_{ave} values remain between 0.0063 and 0.0080. Final part of records NF-P types of NDAs results, the IDR_{ave} values of Case-III structures are examined, the IDR_{ave} values remain between 0.0065 and 0.0079. The IDR_{ave} values of the Case-IV structures are examined, the IDR_{ave} values remain between 0.0086 and 0.010 for FF type TH records of NDAs, and between 0.0083 and 0.098 for NF-NP type TH records of NDAs. Moreover, for NF-P type TH records of NDAs, the IDR_{ave} values stay between 0.0085 and 0.0099 (Figure 8).

Fig. 7 Variation of IDR average along the story for each earthquake group according to sensitivity coefficient (θ) change in outer frames

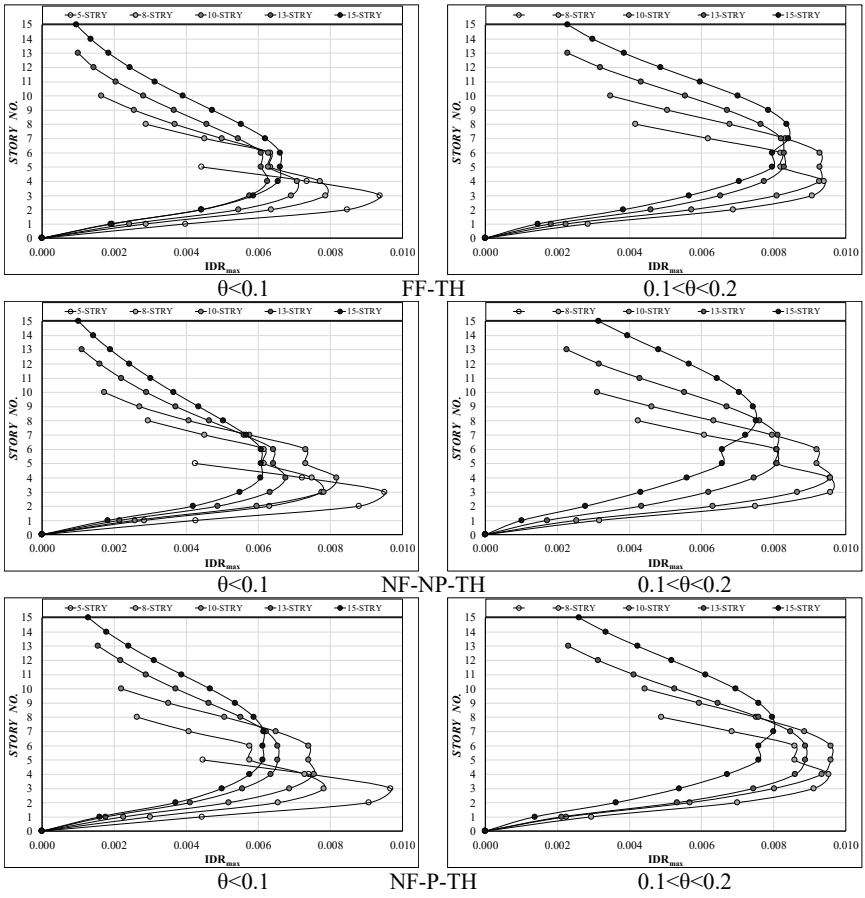

Fig. 8 Variation of the maximum IDR for each earthquake group according to sensitivity coefficient (θ) change in outer frames

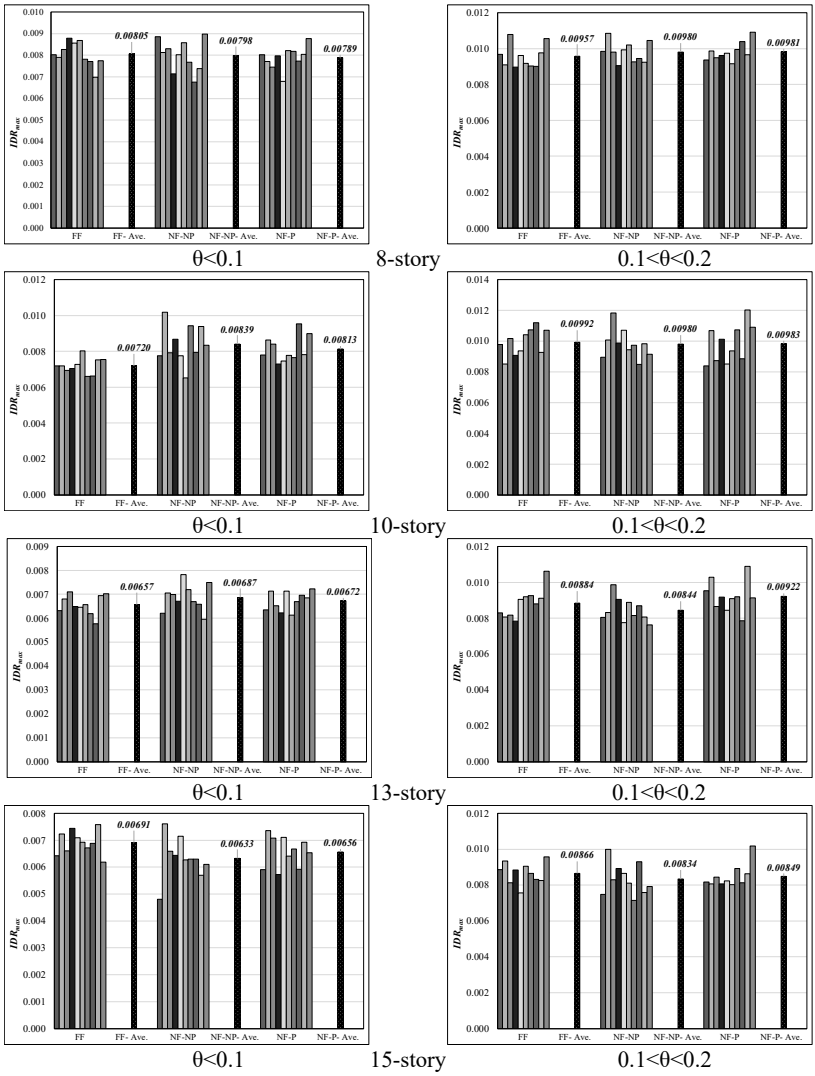

The main variable parameter in the sample structures examined in the study was the change in sensitivity "θ" coefficient. After the structural models were modeled in 3D (all structures are symmetrical), an inner frame in the middle of the structures and a frame from the outside were selected and their behavior was evaluated by NDAs analysis. For NDAs, the series consisting of FF, NF-NP and NF-P type earthquake rockers and with 10 records for each group earthquake were used. The related earthquakes were

matched according to the design spectrum and used in the analysis. As a result, the behavior of the structures was evaluated using IDR coefficients using 4 different frames and 30 earthquake records. According to the data obtained;

- If this coefficient is used in the range of $0<\theta<0.1$, CMRF systems do not reach the IO limit for all earthquake recording types except 8-story CMRF inner frames.
- If this coefficient is in the range of $0.1<\theta\leq0.2$, if this coefficient is used in the relevant range, CMRF systems reach the IO limit for IDR_{max} for all earthquake recording types except 15-story CMRF inner frames.
- In outer frames, if this coefficient is used in the range of $0<\theta<0.1$, all CMRF systems for all earthquake recording types fall below the IO limit for IDR_{max}.
- In outer frames, if it is in the range of $0.1<\theta\leq0.2$, this coefficient exceeds the IO limit for all CMRF systems IDR_{max} in NF-P earthquake records. In other recordings, 8- and 10-story CMRFs reach the IO damage point for IDR_{max}, while the remaining 13- and 15-story CMRF systems reach values very close to the IO limit for IDR_{max}
- In summary, leaving the θ coefficient in this range of $0<\theta<0.1$ creates more reliable results for the IO safety level in earthquakes.

References

Acun, B. (2012). *Eurocode 8: Seismic Design of Buildings, Worked Examples*. Publications Office of the European Union.

Altoontash, A. (2004). Simulation and damage models for performance assessment of reinforced concrete beam-column joints. *PhD Thesis*, *August*, 232.

Antoniou, S., Fragiadakis, M., & Pinho, R. (2008). *Modelling inelastic buckling of reinforcing bars under earthquake loading*. *December*, 347–361. https://doi.org/10.1201/9780203881637.ch22

Baba T, Inai E, Kai M, Noguchi T, M. A. (1995). Structural behaviour of concrete filled steel tubular columns under axial compressive load, part 2: test results on rectangular columns. *Abstracts of the Annual Convention of the Architectural Institute of Japan*, 737–8.

Boukhalkhal, S. H., Ihaddoudène, A. N. T., Da Costa Neves, L. F., & Madi, W. (2019). Dynamic behavior of concrete filled steel tubular columns. *International Journal of Structural Integrity*, *10*(2), 244–264. https://doi.org/10.1108/IJSI-07-2018-0040

Broderick, B. M., & Elnashai, A. S. (1996). Seismic response of composite frames - I. Response criteria and input motion. *Engineering Structures*, *18*(9), 696–706. https://doi.org/10.1016/0141-0296(95)00211-1

Bruneau, M., Uang, C., & Sabelli, R. (2008). Ductile Design of Steel Structures. *Animal Genetics*, *39*(5), 561–563.

Caldara, R. (1998). Composite substructures with partial shear connection: low cycle fatigue behaviour and analysis issues. *Mechanical Engineering*, 1–8.

Castro, J. M. de F. (2006). *Seismic Behaviour of Composite Moment-Resisting Frames*. *April*.

Castro, J. M., Elghazouli, A. Y., & Izzuddin, B. A. (2007). Assessment of effective slab widths in composite beams. *Journal of Constructional Steel Research*, *63*(10), 1317–1327. https://doi.org/10.1016/j.jcsr.2006.11.018

Choi, K. K., & Xiao, Y. (2010). Analytical Studies of Concrete-Filled Circular Steel Tubes under Axial Compression. *Journal of Structural Engineering*, *136*(5), 565–573. https://doi.org/10.1061/(ASCE)ST.1943-541X.0000156

Elghazouli, A. Y., Castro, J. M., & Izzuddin, B. A. (2008). Seismic performance of composite moment-resisting frames. *Engineering Structures*, *30*(7), 1802–1819. https://doi.org/10.1016/j.engstruct.2007.12.004

EN 1994-1-1. (2004). Eurocode 4: Design of composite steel and concrete structures – Part 1-1: General rules and rules for buildings. *European Committee for Standardization*, *3*(February), 33–38. https://doi.org/10.1002/14651858.CD009305.pub2

EN 1998-1. (2004). Eurocode 8: Design of structures for earthquake resistance—Part 1: General rules, seismic actions and rules for buildings. *European Committee for Normalization, Brussels*, *2005*. https://doi.org/[Authority: The European Union per Regulation 305/2011, Directive 98/34/EC, Directive 2004/18/EC]

Etli, S. (2021). *Performance Assessment of Steel-Concrete Composite Buildings* (Issue April) [Ph.D. Thesis]. Gaziantep University.

Etli, S. (2022). Parametric Analysis of the Performance of Steel-Concrete Composite Structures Designed with TBDY 2018. *International Journal of Innovative Engineering Applications*, *6*(1). https://doi.org/10.46460/ijiea.1029942

Etli, S., & Güneyisi, E. M. (2020). Seismic performance evaluation of regular and irregular composite moment resisting frames. *Latin American Journal of Solids and Structures*, *17*(7), 1–22. https://doi.org/10.1590/1679-78255969

Etli, S., & Güneyisi, E. M. (2021). Assessment of Seismic Behavior Factor of Code-Designed Steel–Concrete Composite Buildings. *Arabian Journal for Science and Engineering*, *46*(5), 4271–4292. https://doi.org/10.1007/s13369-020-04913-9

Etli, S., & Güneyisi, E. M. (2022a). Effect of nonlinear modeling approaches used for composite elements on seismic behavior of composite framed buildings. *Sadhana - Academy Proceedings in Engineering Sciences*, *47*(2). https://doi.org/10.1007/s12046-022-01871-w

Etli, S., & Güneyisi, E. M. (2022b). Effect of Using Eccentric Braces with Different Link Lengths on the Seismic Demand of CFST Column-Composite Beam Frames Subjected to Near-Field and Far-Field Earthquakes. In *Iranian Journal of Science and Technology - Transactions of Civil Engineering*. https://doi.org/10.1007/s40996-022-00994-8

FEMA 273, N. (1997). *Guidelines for the seismic rehabilitation of buildings*. Federal Emergency Management Agency Washington, DC.

Filippou, F. C., Popov, E. P., & Bertero, V. V. (1983). Effects of Bond Deterioration on Hysteretic Behaviour of Reinforced Concrete Joints. Report to the National Science Foundation. *Earthquake Engineering Research Center*, *August*, 1–212.

Fukumoto, T., & Morita, K. (2005). Elastoplastic behavior of panel zone in steel beam-to-concrete filled steel tube column moment connections. *Journal of Structural Engineering*, *131*(12), 1841–1853. https://doi.org/10.1061/(ASCE)0733-9445(2005)131:12(1841)

G. Monti, C. Nuti, S. S. (1996). *CYRUS: CYclic Response of Upgraded Sections. A program for the analysis of retrofitted or repaired sections under biaxial cyclic loading including buckling of rebars*.

Güneyisi, E. M., & Etli, S. (2020). Response of steel buildings under near and far field earthquakes. *Civil Engineering Beyond Limits*, *1*(2), 24–30. https://doi.org/10.36937/cebel.2020.002.004

Hawkins, N. M., & Mitchell, D. (1984). Seismic Response of Composite Shear Connections. *Journal of Structural Engineering*, *110*(9), 2120–2136. https://doi.org/10.1061/(ASCE)0733-9445(1984)110:9(2120)

Huang, Z., Huang, X., Li, W., Zhou, Y., Sui, L., & Liew, J. Y. R. (2018). *Experimental behaviour of very high-strength concrete-encased steel composite column subjected to axial compression and end moment*. *Asccs*, 323–329.

Kanatani, H., Tabuchi, M., Kamba, T., Hsiaolien, J., & Ishikawa, M. (1987). A study on concrete filled RHS column to H-beam connections fabricated with HT bolts in rigid frames. *Composite Construction in Steel and Concrete*, 614–635.

Kim, K. D., & Engelhardt, M. D. (2002). Monotonic and cyclic loading models for panel zones in steel moment frames. *Journal of Constructional Steel Research*, *58*(5–8), 605–635. https://doi.org/10.1016/S0143-974X(01)00079-7

Leon, R. T., Hajjar, J. F., Gustafson, M. A., & Shield, C. (1998). Seismic Response of Composite Moment-Resisting Connections. II: Behavior. *Journal of Structural Engineering*, *124*(August), 868–876.

Li, J. T., Chen, Z. P., Xu, J. J., Jing, C. G., & Xue, J. Y. (2018). Cyclic behavior of concrete-filled steel tubular column–reinforced concrete beam frames incorporating 100% recycled concrete aggregates. *Advances in Structural Engineering*, *21*(12), 1802–1814. https://doi.org/10.1177/1369433218755521

Martínez-Rueda, J. E., & Elnashai, A. S. (1997). Confined concrete model under cyclic load. *Materials and Structures*, *30*(3), 139–147. https://doi.org/10.1007/BF02486385

Menegotto, M., & Pinto, P. E. (1973). Method of Analysis for Cyclically Loaded R. C. Plane Frames Including Changes in Geometry and Non-Elastic Behavior of Elements under Combined Normal Force and Bending. *Proceedings of IABSE Symposium on Resistance and Ultimate Deformability of Structures Acted on by Well Defined Loads*, 15–22. https://doi.org/http://dx.doi.org/10.5169/seals-13741

Miranda, B. E. (2012). Strength Reduction Factors in Performance-Based Design. *Ingeniería, Investigación y Tecnología*, 35–39. https://doi.org/10.4156/ijact.vol5.issue9.136

Muhummud, T. (2003). *Seismic behavior and design of composite SMRFs with concrete filled steel tubular columns and steel wide flange beams.* 551.

Nogueiro, P., Simoesdasilva, L., Bento, R., & Simoes, R. (2005). Numerical implementation and calibration of a hysteretic model with pinching for

the cyclic response of steel and composite joints. *Fourth International Conference on Advances in Steel Structures*, 767–774. https://doi.org/10.1016/b978-008044637-0/50112-8

Plumier, A. (2000). European research and code developments on seismic design of composite steel concrete structures. *12 World Conference on Earthquake Engineering--Conference Proceeding*, 1–8.

Seismosoft. (2016). *SeismoStruct A computer program for static and dynamic nonlinear analysis of framed structures V 7.0*.

Shahrooz, B. M., Pantazopoulou, S. J., & Chern, S. P. (1993). Modeling slab contribution in frame connections. *Journal of Structural Engineering*, *118*(9), 2475–2494. https://doi.org/10.1061/(ASCE)0733-9445(1992)118

Srinivasan, C. N., & Schneider, S. P. (1999). Axially Loaded Concrete-Filled Steel Tubes. *Journal of Structural Engineering*, *125*(10), 1202–1206. https://doi.org/10.1061/(ASCE)0733-9445(1999)125:10(1202)

Susantha, K. A. S., Ge, H., & Usami, T. (2001). Uniaxial stress-strain relationship of concrete confined by various shaped steel tubes. *Engineering Structures*, *23*(10), 1331–1347. https://doi.org/10.1016/S0141-0296(01)00020-7

Thermou, G. E., Elnashai, A. S., Plumier, A., & Done, C. (2004). Seismic design and performance of composite frames. *Journal of Constructional Steel Research*, *60*(1), 31–57. https://doi.org/10.1016/j.jcsr.2003.08.006

Tomii, M., Yoshimura, K., & Morishita, Y. (1977). Experimental Studies on Concrete-Filled Steel Tubular Stub Columns Under Concentric Loading. *International Colloquium on Stability of Structures Under Static and Dynamic Loads*, 718–741.

Uy, B. (2001). Strength of short concrete filled high strength steel box columns. *Journal of Constructional Steel Research*, *57*(2), 113–134. https://doi.org/10.1016/S0143-974X(00)00014-6

Vision 2000, Conceptual Framework for Performance Based Seismic Engineering of Buildings. (1995). *Structural Engineers Association of California*, *2*.

Xiao, Y., & Wu, H. (2000). Compressive behavior of concrete confined by carbon fiber composite jackets. *Journal of Materials in Civil Engineering*, *12*(2), 139–146.

Xu, J. J., Chen, Z. P., Ozbakkaloglu, T., Zhao, X. Y., & Demartino, C. (2018). A critical assessment of the compressive behavior of reinforced recycled aggregate concrete columns. *Engineering Structures*, *161*(January), 161–175. https://doi.org/10.1016/j.engstruct.2018.02.003

Zhang, X., & Gao, X. (2019). The hysteretic behavior of recycled aggregate concrete-filled square steel tube columns. *Engineering Structures*, *198*(April), 109523. https://doi.org/10.1016/j.engstruct.2019.109523